RESEARCH

Open Access

SN38-loaded nanomedicine mediates chemo-radiotherapy against CD44-expressing cancer growth

Shu-Jyuan Yang[1†], Jui-An Pai[1†], Cheng-Jung Yao[1,2], Chung-Huan Huang[1], Jenny Ling-Yu Chen[3], Chung-Hao Wang[4], Ke-Cheng Chen[1,5*] and Ming-Jium Shieh[1,6*]

†Shu-Jyuan Yang and Jui-An Pai are contributed equally to this work

*Correspondence:
CSKChen@gmail.com;
soloman@ntu.edu.tw

[1] Institute of Biomedical Engineering, College of Medicine and College of Engineering, National Taiwan University, No. 1, Section 1, Jen-Ai Road, Taipei 100233, Taiwan
[2] Division of Gastroenterology, Department of Internal Medicine, Wan Fang Hospital, Taipei Medical University, No. 111, Section 3, Xinglong Road, Taipei 116079, Taiwan
[3] Department of Radiology, National Taiwan University Hospital and College of Medicine, No. 7, Chung-Shan South Road, Taipei 100233, Taiwan
[4] Gene'e Tech Co. Ltd, 2F., No. 661, Bannan Rd., Zhonghe Dist., New Taipei City 235, Taiwan
[5] Department of Surgery, National Taiwan University Hospital and College of Medicine, No. 7, Chung-Shan South Road, Taipei 100233, Taiwan
[6] Department of Oncology, National Taiwan University Hospital and College of Medicine, No. 7, Chung-Shan South Road, Taipei 100233, Taiwan

Abstract

Background: Chemo-radiotherapy is the combined chemotherapy and radiotherapy on tumor treatment to obtain the local radiosensitization and local cytotoxicity of the tumor and to control the microscopic metastatic disease.

Methods: In this study, 7-ethyl-10-hydroxycamptothecin (SN38) molecules could be successfully loaded into human serum albumin (HSA)–hyaluronic acid (HA) nanoparticles (SH/HA NPs) by the hydrophobic side groups of amino acid in HSA.

Results: HSA could be used to increase the biocompatibility and residence time of the nanoparticles in the blood, whereas HA could improve the benefits and overall treatment effect on CD44-expressing colorectal cancer (CRC), and reduce drug side effects. In addition to its role as a chemotherapeutic agent, SN38 could be used as a radiosensitizer, able to arrest the cell cycle, and allowing cells to stay in the G2/M stage, to improve the sensitivity of tumor cells to radiation. In vivo results demonstrated that SH/HA NPs could accumulate in the tumor and produce significant tumor suppression, with no adverse effects observed when combined with γ-ray irradiation. This SH/HA NPs-medicated chemo-radiotherapy could induce an anti-tumor immune response to inhibit the growth of distal tumors, and produce an abscopal effect.

Conclusions: Therefore, this SN38-loaded and HA-incorporated nanoparticle combined with radiotherapy may be a promising therapeutic artifice for CRC in the future.

Keywords: Chemo-radiotherapy, 7-Ethyl-10-hydroxycamptothecin, Human serum albumin, Hyaluronic acid, Abscopal effect

Introduction

Colorectal cancer (CRC) is one of the leading cause of cancer death worldwide, and its incidence is currently increasing rapidly. The establishment of multifunctional therapeutic medicine is critical to address the challenging problems associated with CRC (Moreno et al. 2016; Attisano and Wrana 2012). Chemo-radiotherapy is the combined chemotherapy and radiotherapy on cancer treatment to obtain the local radiosensitization and local cytotoxicity of the tumor and to control the microscopic metastatic

disease (DuRoss et al. 2021). Chemo-radiotherapy can be used to decrease cancer size before surgery, making tumors easier to remove. Radiation ablates tumor cells to lead to molecular changes, including cellular adhesion molecules and inflammatory cytokines, such as various radioactive elements or dangerous-related molecular-pattern molecules (DAMP) and induce immune effect (Corso et al. 2011; Kanegasaki et al. 2014).

Radiosensitizers can enhance the sensitivity of tumors to radiation and improve their curative effect by increasing radiation-induced oxygen free radicals and DNA damage. In recent years, the camptothecin-derived drugs have been proved to possess radio-sensitization effects on cancer cells, by inhibiting the function of DNA topoisomerase I in intracellular DNA repair to lead to a significant G2/M phase arrest, followed by increased apoptosis (Wang et al. 2018). CPT-11, a camptothecin-derived drug for the treatment of CRC, kills cancer cells mainly through inhibition of DNA topoisomerase I, reducing the capability of cancer cells to produce required proteins and leading to eventual death from apoptosis (Armand et al. 1995; Magrini et al. 2002). The compound 7-ethyl-10-hydroxycamptothecin (SN38), the activated form of CPT-11, has about 200 times the activity of CPT-11 (Bala et al. 2013) and also displays as a radiosensitizer during radiation therapy, to kill cells in a short time. The encapsulation of SN38 in nanoparticles, polymer–drug conjugates, and liposomes has been attempted, to solve its application challenge in pharmaceutical formulations in recent years (Rivory et al. 1996; Zhang et al. 2004; Roger et al. 2011, Venditto and Szoka 2013). However, the synthesis of SN38-loaded carriers was too complicated to permit manufacture on a large scale and often required the use of toxic agents or organic solvents.

Conventional pharmaceuticals have poor bioavailability and relatively fast clearance from the human body, leading to the need of high-dose drug intake that may cause the potential adverse effects on humans and the environment (Lam et al. 2015). To reduce the side effects of drugs entering the environment, and produce therapeutic effects using a low dose of medication, nanomedicine, a medical application of nanotechnology, has many advantages over conventional pharmaceuticals. These advantages include improved drug bioavailability and therapeutic efficiency at reduced doses and at low frequency; targeting specific tissues; prolonged storage life; and increased patient compliance and convenience (Orive et al. 2003). However, nanoparticles can cause nanotoxicity and may lead to health and environmental risks by interacting with both natural and anthropogenic chemicals (Wang et al. 2014). To reduce the potential toxicity of nanoparticles, the selection of biodegradable materials and non-toxic ingredients in the development of nanosystems is important. The idea of green chemistry can be applied in the nano-drug delivery system design and establishment, for selecting biodegradable materials, non-toxic ingredients, and safe manufacturing processes, to reduce or eliminate the use and production of hazardous substances (Clark et al. 2014).

Human serum albumin (HSA) has been developed as a carrier for hydrophobic chemotherapeutics for many years. The drug that has attracted the most attention is the taxol-serum albumin nano-carrier under the trade name Abraxane® (Kouchakzadeh et al. 2015). HSA can bind glycoprotein (gp60) on the surface of vascular endothelial cells, and regulate the transcytosis of HAS-binding molecules to enter the interstitial region of the tumor site. By combining extracellular matrix glycoproteins expressed in large quantities on tumor cells, HSA-based nano-carriers can be easily uptaken by tumor cells to
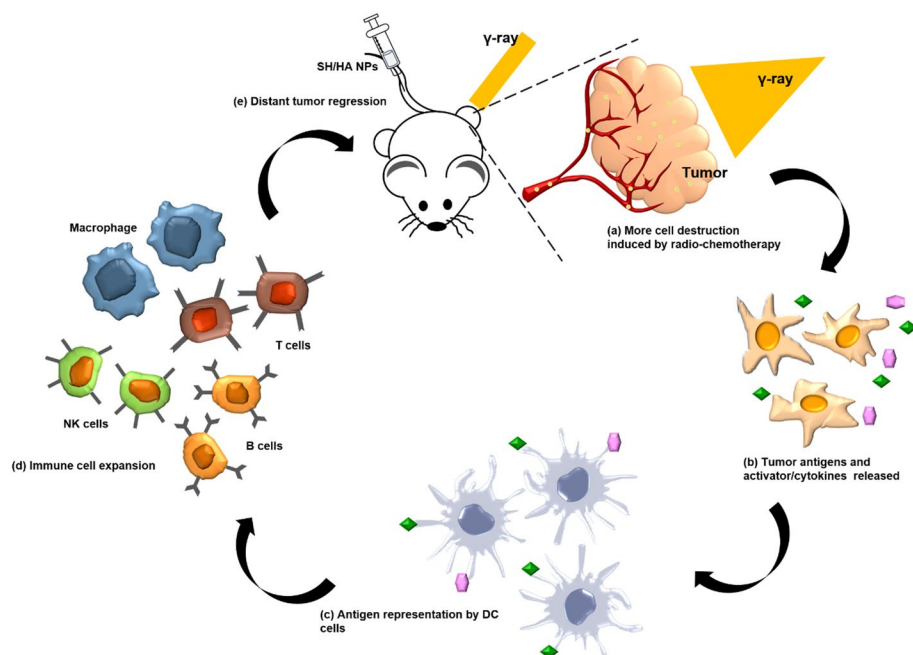
Scheme 1 Schematic representation of the SH/HA NPs combined with radiation on colorectal cancer treatment and immune cell infiltrates

improve the treatment effect and reduce the side effects of chemotherapy drugs (Frei 2011; Kim et al. 2011; Quan et al. 2011; Elsadek and Kratz 2012; Ding et al. 2014; Sheng et al. 2014). HSA can also effectively enhance the biocompatibility and circulation time of nano-carriers in the blood (Tirkey et al. 2017; Lee et al. 2018). Hyaluronic acid (HA) is a natural linear glycosaminoglycan polymer polymerized by D-glucuronic acid and N-acetyl-D-glucosamine. Owing to its biocompatibility, enzyme degradability, and effective tumor-targeting ability, it has attracted considerable attention. Its receptor, CD44, is a non-kinase transmembrane glycoprotein, which is overexpressed in different strains of cancer cells including cancer stem cells (CSCs) (Yin et al. 2016), and is related to tumor development, invasion, and metastasis. Various HA-related drug delivery systems have recently been developed for CD44-regulated tumor target therapy (Cadete and Alonso 2016; Jiang et al. 2021; Hu et al. 2020).

In our previous study, we have successfully encapsulated SN38 in HSA-based carriers and established gold nanoshells on this carrier surface for chemo-photothermal therapy on CRC, but this nanoparticle lacked tumor target properties, which might result in unexpected adverse effects (Yang et al. 2022). In this study, we encapsulated SN38 in HSA/HA nanoparticles by the lyophilization–hydration method, which not only provided a simple and safe manufacturing processes, but also eliminated the use and production of hazardous substances. The use of HSA shall increase the biocompatibility and circulation time of hydrophobic drug SN38 in blood, and the HA can target and increase the uptake of SN38-loaded nanoparticles in CD44-expressing tumor cells to improve the chemo-radiotherapy effect and reduce the toxicity of chemotherapy drugs. In addition, the immune cells response induced by chemo-radiotherapy on distal tumor growth suppression was also investigated in a murine model (Scheme 1).

Materials and methods

Materials

HSA ($\geq 96\%$), HA (MW = 500 kDa), Fluorescein 5(6)-isothiocyanate (FITC), 3-(4,5-dimethylthiazol-2-yl)-2,5-diphenyltetrazolium bromide (MTT), and dimethyl sulfoxide (DMSO) were purchased from Sigma-Aldrich (USA). 7-Ethyl-10-hydroxycamptothecin (SN38) was acquired from ScinoPharm Taiwan, Ltd. (Tainan, Taiwan). Tali™ Cell Cycle Kits were purchased from Thermo Fisher Scientific (Waltham, MA, USA). The chemotherapeutic injection solution used in the clinic, CAMPTO®, was acquired from Pfizer Perth Pty. Ltd. (Australia).

Preparation of SN38-encapsulated and HA-incorporated nanoparticles (SH/HA NPs)

SH/HA NPs were prepared using a lyophilization–hydration method established for the hydrophobic drug-encapsulated micelles in our previous studies (Peng et al. 2008; Tsai et al. 2017). The preparation process can be briefly described as follows: 0.5 mg SN38 powder was well-dissolved in 1 mL of DMSO, and then the HSA–HA mixture was added into the solution at an SN38/HSA/HA weight ratio of 1/11/0.069. The SN38/HSA/HA mixture was dispersed in 1 mL of Gitose injection 5% solution (dextrose 5% solution, Nang Kuang Pharmaceutical Co. Ltd., Taiwan) after lyophilization, and was ultrasonicated to form SH/HA NPs. SH NPs were prepared according to the method described above, but without the incorporation of HA. The prepared nano-carrier solutions were used directly without treatment.

Characterization of SH/HA NPs

The hydrodynamic size and zeta potential of the prepared SH and SH/HA NPs were carried out using a Zetasizer Nano-ZS90 (Malvern Instruments Ltd, UK). The surface morphology of SH and SH/HA NPs was observed under a transmission electron microscope (TEM, Hitachi H-7500, Tokyo, Japan) after the precipitation of SH and SH/HA NPs on dried carbon-coated copper grids. Powder X-ray diffraction (XRD) patterns of SN38, HA, HSA, SH NPs, and SH/HA NPs were recorded on a D2 PHASER X-ray diffractometer (Bruker AXS Inc., WI, USA) equipped with Cu Kα radiation ($\lambda = 1.5418$ Å).

The loading efficiency of SN38 in the prepared SH and SH/HA NPs was determined using high-performance liquid chromatography (HPLC, Waters e2696). The un-loaded SN38 was removed from the prepared SH or SH/HA NP solution by filtrating through a 0.22 μm filter unit (Merck Millipore Ltd., Tullagreen, Ireland), and then the filtered particle solution was re-dissolved in DMSO and injected into the HPLC system. The elution mode consisting of 0.1% trifluoroacetic acid and acetonitrile (v/v = 60/40) as the mobile phase at a flow rate of 1 mL/min was used. The separation was performed on a Waters Symmetry® C18 reversed-phase column (XBridgeTM) with fluorescent detection of SN38 at 365/550 nm. The SN38 encapsulation efficacy (EE) and drug-loading content (DC) in the nanoparticles was calculated using the following equations:

$$EE\ (\%) = \text{Weight of SN38 in the particles/Total weight of feeding SN38} \times 100\%$$

$$DC\ (\%) = \text{Weight of SN38 in the particles/Total weight of particles} \times 100\%$$

The storage stability of the nanoparticles is important and must be considered during design and development of pharmaceutical formulations (Gradauer et al. 2013). For this purpose, the prepared SH NPs or SH/HA NPs were re-lyophilized and then preserved at 4 °C. At 1, 10, 20, and 30 days, 1 mL ddH$_2$O was added into the re-lyophilized SH NPs or SH/HA NPs, and the particle size was determined using a Zetasizer Nano-ZS90.

Determination of CD44 antigen expression on cell surface

A human colon cancer cell line derived from a lymph node metastatic site, SW620, and a human colon cancer cell line, HT29, were cultivated in Dulbecco's modified Eagle's medium (DMEM) supplemented with 10% fetal bovine serum (FBS) and 1% Gibco® antibiotic–antimycotic solution, respectively. The other human colon cancer cell line, HCT116, was cultivated in McCoy's 5a medium with 10% FBS and 1% Gibco® antibiotic–antimycotic solution. They were all cultured at 37 °C in an atmosphere of 5% CO$_2$, and culture media were changed on alternate days.

Once SW620, HT29, and HCT116 cells were cultured to 80% confluency, each cell line was detached using the Gibco™ Trypsin/EDTA Solution (TE) solution, counted, and then re-suspended in 500 μL of cold flow cytometry buffer (PBS containing 10% FBS and 1% sodium azide). At least 1×10^6 cells were incubated with 10 μL PE anti-human CD44 antibody (BioLegend, Inc., CA, USA) on ice for 30 min in the dark. After being washed with cold flow cytometry buffer, the labeled cells were re-suspended in 500 μL flow cytometry buffer and determined by a flow cytometry with the BD FACSCalibur system (Becton & Dickinson, Mountain View, CA, USA).

Cellular uptake and in vitro cytotoxicity of SH/HA NPs

Glass plates were placed in 6-well plates and seeded with SW620, HT29, or HCT116 cells. After 24 h, the medium was replaced with fresh medium containing the FITC-modified SH NPs and SH/HA NPs. To investigate the effect of HA−CD44-mediated endocytosis, the cells were pre-treated with 0.1 mg/mL HA for 1 h and then fed with FITC-modified SH/HA NPs. After further 6 h cultivation, the glass plate was washed three times with PBS, fixed with 10% formalin, and then examined under a spectral confocal and multiphoton system (Leica TCS SP8, Wetzlar, Germany). The average FITC fluorescent intensity of six regions obtained from randomly chosen areas in cells was analyzed using the Leica Application Suite X software (Leica Microsystems Inc., Illinois, USA) to determine the uptake of nanoparticles. The green brightness of the FITC-SH NPs treated group was designated as 100% for the individual colon cancer cell lines (Yang et al. 2020).

SW620, HT29, or HCT116 cells were separately seeded into 96-well plates at a density of 5×10^3 cells/well. After 24 h cultivation, the cells were washed with PBS and then incubated in fresh medium containing SN38, SH NPs, and SH/HA NPs at SN38 concentrations of 0, 5, 10, and 100 ng/mL, respectively. After 48 h, the cell viability was determined by MTT assay, and the cell viability was expressed as a percentage relative to that of the control group.

Cell cycle analysis

4×10^5 cells/well of SW620 and HT29 cells were seeded in 6-well plates and incubated overnight at 37 ℃. The cells were exposed to free SN38, SH NPs, and SH/HA NPs at an SN38 dose of 5 ng/mL for 48 h. The alive cells were collected and fixed in 70% ethanol for an hour, followed by treatment with Tali™ Cell Cycle Kits (Thermo Fisher Scientific, Catalog No. A10798), according to the manufacturer's instructions. Finally, cell cycle distribution and regulation were determined using BD FACSCalibur system, with PBS-treated cells used as the negative control.

In vitro cytotoxicity of combined chemo-radiotherapy

The in vitro anticancer effects of combined chemo-radiotherapy with SH NPs or SH/HA NPs were assessed using MTT assay. SW620 and HT29 cells with a cell density of 5×10^3 cells/well were seeded in 96-well plates and incubated for 24 h. The cells were then washed with PBS and cultivated in media containing SN38, SH NPs, and SH/HA NPs at SN38 concentrations of 0, 5, 10, and 100 ng/mL, respectively. After 48 h exposure, cells were irradiated with γ-rays at 6 Gy. All cells were incubated for another 48 h, and then the cell viability was determined by MTT assay and expressed as a percentage relative to that of the control (only PBS-treated) group.

In vivo anticancer efficacy of combined chemo-radiotherapy from SH/HA NPs plus irradiation

Four-week-old Female BALB/CAnN.Cg-Foxn1nu/CrlNarl nude mice were acquired from the National Laboratory Animal Center (Tainan, Taiwan). In vivo animal experiments were performed at Laboratory Animal Center of National Taiwan University College Medicine with prior Institutional Animal Care and Use Committee (IACUC) approval. HT29 xenograft tumors were produced by subcutaneous injection of 1×10^7 cells in 150 μL PBS at the front flank to form distal tumors and the hind flank close to the leg to form primary tumors, respectively. The tumor length (l) and width (w) were measured every two days, and the volume (V) was calculated using the formula $V = lw^2/2$.

When the tumor volume at the hind flank achieved to 50–100 mm^3, the tumor-bearing mice were randomly divided into seven groups (n = 5 in each group), and treated with (a) saline; (b) the drug, CAMPTO® (20 mg of CPT-11/kg); (c) SH NPs (20 mg of SN38/kg); (d) SH/HA NPs (20 mg of SN38/kg); (e) SH NPs (20 mg of SN38/kg) plus γ-ray irradiation; (f) SH/HA NPs (20 mg of SN38/kg) plus γ-ray irradiation; or (g) saline plus γ-ray irradiation. The mice were intravenously injected once on day 0. The primary tumor in the hind flank was exposed to 6 Gy of γ-radiation 24 h post injection for the radiation-treated groups. The tumor sizes and body weights of the mice were measured and recorded every 2 to 3 days for 28 days. At the end of the experimental period, the mice were sacrificed, and the tumor and main organ tissues (heart, liver, spleen, lung, and kidney) were excised and fixed in 10% paraformaldehyde solution for histopathological tests.

To investigate the distribution of the prepared nanoparticles in the mice, Cy7.0-labeled SH NPs and SH/HA NPs were intravenously injected into HT29 tumor-bearing mice. At

3 and 24 h post injection, the tumor, heart, liver, spleen, lung, and kidney tissues were excised and imaged using an IVIS Imaging System Spectrum Instrument (Xenogen, Caliper Life Sciences Inc).

Effect of combined chemo-radiotherapy from SH/HA NPs plus irradiation on immune cell response on distal tumors

To investigate the immune cell response on distal tumors (non-irradiated tumors), the tumor-bearing mice were intravenously injected with saline, CAMPTO®, SH NPs or SH/HA NPs, and exposed to 6 Gy of γ-radiation on primary tumors 24 h post injection. The distal tumors of the mice were collected 72 h after treatment with γ-radiation and cut into several portions. The tumor samples were digested using a 1 mg/mL collagenase solution at 37 °C for 30 min and then passed twice through 70 μm nylon cell strainers into single cell suspensions. The cells were washed twice with PBS and incubated in 1 mL staining solution (PBS containing 10% FBS, 1% sodium azide, and fluorescently labeled antibodies) on ice for 30 min in the dark. The fluorescently labeled antibodies used here were CD19-AlexaFlour488, CD11c-FITC, F4/80-FITC, DX5-APC, and CD3-PE (Biolegend, San Diego). The samples were analyzed using flow cytometry with the BD FACSCalibur platform (Tremble et al. 2019).

Statistical analysis

The experimental data are presented as the mean ± standard deviation (S.D.). The S.D. was obtained using the following equation:

$$\sigma = \frac{\sqrt{\sum (Xi - \mu)}}{N}$$

where σ is S.D., N is the sample number, X_i is each value from sample, and μ is the mean value. One-way ANOVA tests were performed to analyze the significance of the differences between groups. A p value lower than 0.05 was considered to be statistically significant.

Results

Synthesis and characterization of SH/HA NPs

SH NPs and SH/HA NPs were developed using a lyophilization–hydration method (Fig. 1A). TEM images showed that the SH NPs or SH/HA NPs had an irregular surface shape, with a particle size of 150–180 nm (Fig. 1B). The average hydrodynamic diameter and zeta potential of the prepared nanoparticles determined by a Zetasizer Nano-ZS90 were as approximately 168 nm and −20 mV, respectively, in dextrose 5% solution, regardless of the incorporation of HA (Table 1). Compared with SH NPs, SH/HA NPs had a broad distribution of sizes (Fig. 1C). The EE values of SN38 in SH NPs and SH/HA NPs were 94.1% and 94.8%, respectively; the DC values of SN38 in SH NPs and SH/HA NPs were 7.87% and 7.90%, respectively.

Because SN38 is hydrophobic and crystalline, its XRD pattern can be utilized to determine the state of SN38 in SH NPs and SH/HA NPs. As shown in Fig. 1D, the sharp peaks in the diffraction pattern of SN38 indicated its strong crystallization but disappeared in the diffraction pattern of SH NPs and SH/HA NPs. The stability of SH NPs or SH/HA
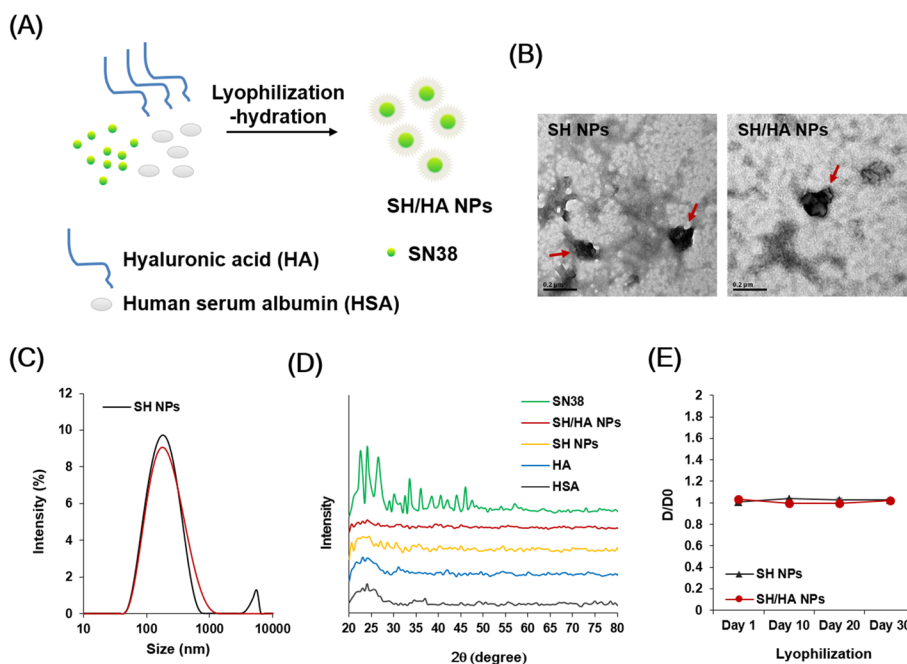
Fig. 1 Characteristics of the SH NPs and SH/HA NPs. **A** SH NPs and SH/HA NPs were prepared using the lyophilization–hydration method. **B** Transmission electron microscopy (TEM) images of SH NPs and SH/HA NPs (red arrow). Samples were negatively stained with 2% uranyl acetate (UA) before imaging. Scale bar = 200 nm. **C** Size distribution of SH NPs and SH/HA NPs. **D** X-ray diffraction patterns of SN38, SH/HA NPs, SH NPs, HA, and HSA. **E** Storage stability of SH NPs or SH/HA NPs was determined by solving the re-lyophilized SH NPs or SH/HA NPs in 1 mL ddH$_2$O at 1, 10, 20, and 30 days ($n = 3$)

Table 1 Characteristics of SH NPs and SH/HA NPs

Sample	Average size (nm)	PDI	Zeta potential (mv)	LD (%)	DC (%)
SH NPs	168.1 ± 1.98	0.236	− 20.1 ± 0.80	94.1 ± 4.29	7.87 ± 0.359
SH/HA NPs	164.3 ± 4.56	0.261	− 20.4 ± 0.89	94.8 ± 5.26	7.90 ± 0.483

NPs was determined by dissolving the re-lyophilized SH NPs or SH/HA NPs in 1 mL ddH$_2$O and then determining the particle size distribution. As shown in Fig. 1E, no significant changes in particle size were found for SH NPs and SH/HA NPs even when they were re-lyophilized and stored at 4 °C for 30 days, indicating the excellent stability in the design and development process of the formulation. These results indicated that the encapsulated SN38 in HSA–HA-based nanoparticles (SH/HA NPs) via a lyophilization–hydration method without the use of toxic organic agents has been successfully established to reduce the potential adverse effects on humans and the environment.

Determination of CD44 antigen expression and cellular uptake of SH/HA NPs

To investigate the uptake of nanoparticles positively correlated with CD44 expression, three colon cancer cell lines, SW620, HT29, and HCT116, were stained with CD44 antibody and then analyzed using flow cytometry. As shown in Fig. 2A, the expression levels of CD44 in HCT116 cells was 97%, and that in HT29 cells was

(A)

(B)

(C)
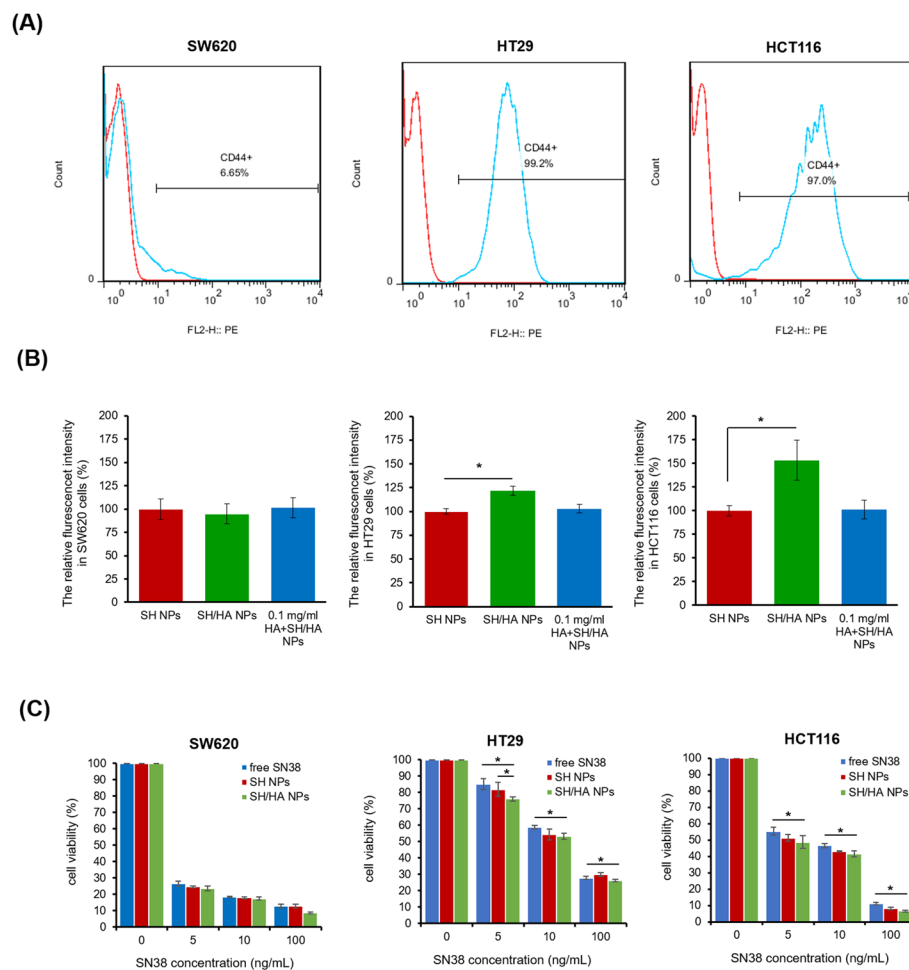
Fig. 2 **A** Expression of CD44 antigen on SW620, HT29, and HCT116 cells determined by flow cytometry. **B** Relative fluorescent intensity of FITC in SW620, HT29, and HCT116 cells ($n = 3$). **C** Viability of SW620, HT29, and HCT116 cells after treated with SN38, SH NPs, and SH/HA NPs at different SN38 concentrations for 48 h ($n = 3$).*$p < 0.05$

99.2%, whereas that in SW620, the negative control, was only 6.65%. Cells with higher CD44 expression may exhibit higher SH/HA NPs-binding affinity and up-take. Additional file 1: Fig. S1 shows the fluorescence of FITC observed under a spectral confocal and multiphoton system in SW620, HT29, and HCT116 cells, which were exposed to FITC-modified SH NPs or SH/HA NPs for 6 h. The green brightness of FITC increased significantly in the HA-incorporated nanoparticles in HT29 or HCT116 cells with high CD44 expression, in comparison with that in SW620 cells with low CD44 expression. When cells were pre-treated with 0.1 mg/mL free HA for 1 h and then fed with SH/HA NPs, there were no statistically significant differences in FITC florescence between the SH NPs- and SH/HA NPs-treated groups, indicating that free HA molecules could compete with SH/HA NPs for CD44 and suppress the HA-mediated recognition of CD44 on the tumor cell surface. As shown in Fig. 2B, HT29 and HCT116 cells fed with HA-incorporated nanoparticles (SH/HA NPs) exhibited a significant FITC fluorescent intensity. These results also indirectly confirmed that HA

was successfully incorporated into SH/HA NPs and could be used as targeting ligand for active targeting of CD44-enriched cancer cells.

The in vitro cytotoxicity of SH NPs or SH/HA NPs compared to that of free SN38 was estimated in SW620, HT29, and HCT116 cells, using an MTT assay. As shown in Fig. 2C, both SH NPs and SH/HA NPs caused cytotoxicity of colorectal cancer cell in a dose-dependent manner. The viability of SW620 cells treated with SH NPs or SH/HA NPs was the same as that of cells treated with free SN38 at SN38 concentrations equivalent to 5, 10, and 100 ng/mL. However, the viability of HT29 or HCT116 cells treated with SH NPs and SH/HA NPs was lower than that of cells treated with free SN38. At a low SN38 concentration (5 ng/mL), the SH/HA NPs-treated HT29 cells displayed more cytotoxicity than did the SH NPs-treated cells. However, at high SN38 concentrations (10 and 100 ng/mL), the difference in the cytotoxicity of HT29 cells induced by SH/HA NPs was similar to that induced by SH NPs. Moreover, the CD44-enriched HT29 cells exhibited more SN38 resistance, but CD44 low-expressing SW620 cell displayed more sensitive to the SN38 toxicity, indicating that SN38 resistance of cancer cells was related to their CD44 level of expression. Because HT29 cells exhibited more SN38 resistance than did HCT116 cells, we only used HT29 cells as CD44-overexpressing cells in the following experiments.

Cell cycle analysis

To evaluate the ability of SN38 to arrest the cell cycle, SW620 and HT29 cells were treated with free SN38, SH NPs, or SH/HA NPs for 48 h, and the cell cycle changes were analyzed using flow cytometry. As shown in Fig. 3, in the untreated SW620 and HT29 cells, the percentage of cells in the G2/M phase were a small percentage (around 10–15%), but the percentage of SW620 and HT29 cells in the G2/M phase achieved to around 70% when treated with free SN38. The percentage of HT29 cells in the G2/M phase was up to 85% after treatment with SH/HA NPs. These results indicated that the prepared nanoparticles could retain the SN38 ability to achieve G2/M phase arrest in SW620 and HT29 cells.
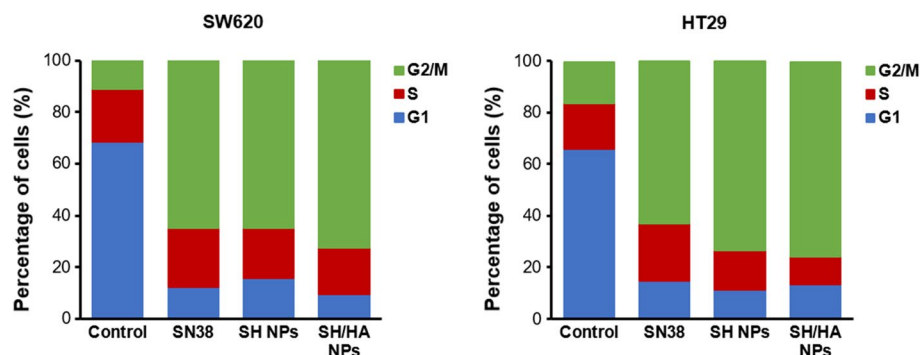
Fig. 3 Cell cycle determination of SW620 and HT29 cells treated with free SN38, SH NPs, and SH/HA NPs at the SN38 dose of 5 ng/mL for 48 h ($n = 3$)

In vitro cytotoxicity of chemo-radiotherapy

The results described above indicated SH NPs and SH/HA NPs could successfully retain the SN38 ability to achieve G2/M phase cell cycle arrest, which should make SW620 and HT29 cells more susceptible to radiation damage. To assess the in vitro effect of the chemo-radiotherapy, the viability of the SW620 and HT29 cells after treatment with free SN38, SH NPs and SH/HA NPs following γ-ray irradiation at 6 Gy were determined using MTT assays. As shown in Fig. 4, no significant difference in cytotoxicity could be observed when SW620 cells were treated with free SN38, SH NPs, and SH/HA NPs with or without γ-ray irradiation at SN38 concentrations of 5, 10, and 100 ng/mL. However, when free SN38-, SH NPs-, or SH/HA NPs-treated HT29 cells at SN38 concentrations of 0, 5, and 10 ng/mL were irradiated with γ-rays, a significant cytotoxicity was observed in comparison with cells without γ-ray irradiation treatment, and the difference in cytotoxicity induced by γ-ray irradiation occurred in an SN38 dose-inverse-dependent manner. At a high SN38 concentration (100 ng/mL), the cytotoxicity caused by radiation was insignificant. The half maximal inhibitory concentrations (IC_{50}) of free SN38, SH NPs, and SH/HA NPs toward HT29 cells were 25.51, 23.96, and 20.01 ng/mL, respectively. The IC_{50} of free SN38 plus γ-ray irradiation was 15.62 ng/mL, whereas that of SH NPs and SH/HA NPs combined with γ-ray irradiation was 9.98 and 8.7 ng/mL, respectively, indicating that the anti-tumor effect of chemo-radiotherapy on HT29 cells could be improved by the HSA-complexed and HA-incorporated nanoparticles (SH/HA NPs).

In vivo antitumor efficacy

To determine the distribution of SH NPs and SH/HA NPs in HT29 tumor-bearing mice, the mice were intravenously injected with Cy7.0-labeled SH NPs and SH/HA NPs, and then the main organ and tumor tissues were excised and observed under an IVIS Imaging System Spectrum Instrument. Because the liver plays as a biological filtration system, and 30–99% of administered nanoparticles will be captured and isolated in the liver from the bloodstream (Zhang et al. 2016). As shown in Fig. 5A, the liver tissues showed a strongest fluorescent intensity at 3 h post injection with either SH NPs or SH/HA NPs. After 24 h post injection, the red intensity in tumor tissues was higher than that in other organ tissues. Moreover, the SH/HA NPs-treated tumor tissue exhibited a significant fluorescence intensity of Cy7.0, which might be contributed by the incorporation of HA
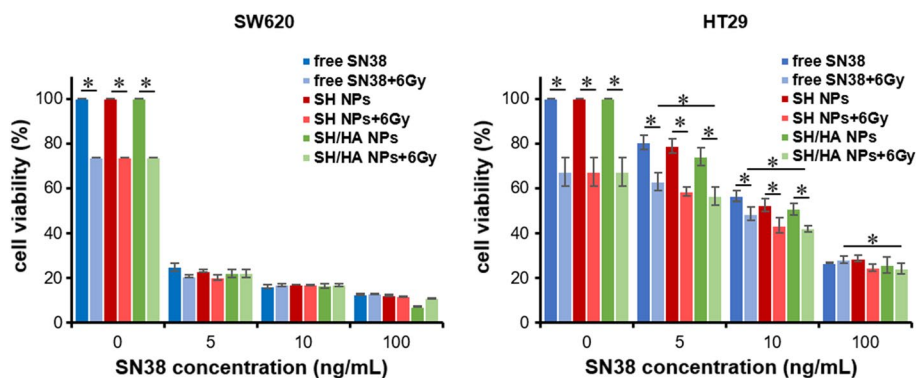
Fig. 4 Viability of SW620 and HT29 cells treated with free SN38, SH NPs, and SH/HA NPs at different SN38 concentrations and γ-ray (6 Gy) ($n = 3$). *$p < 0.05$
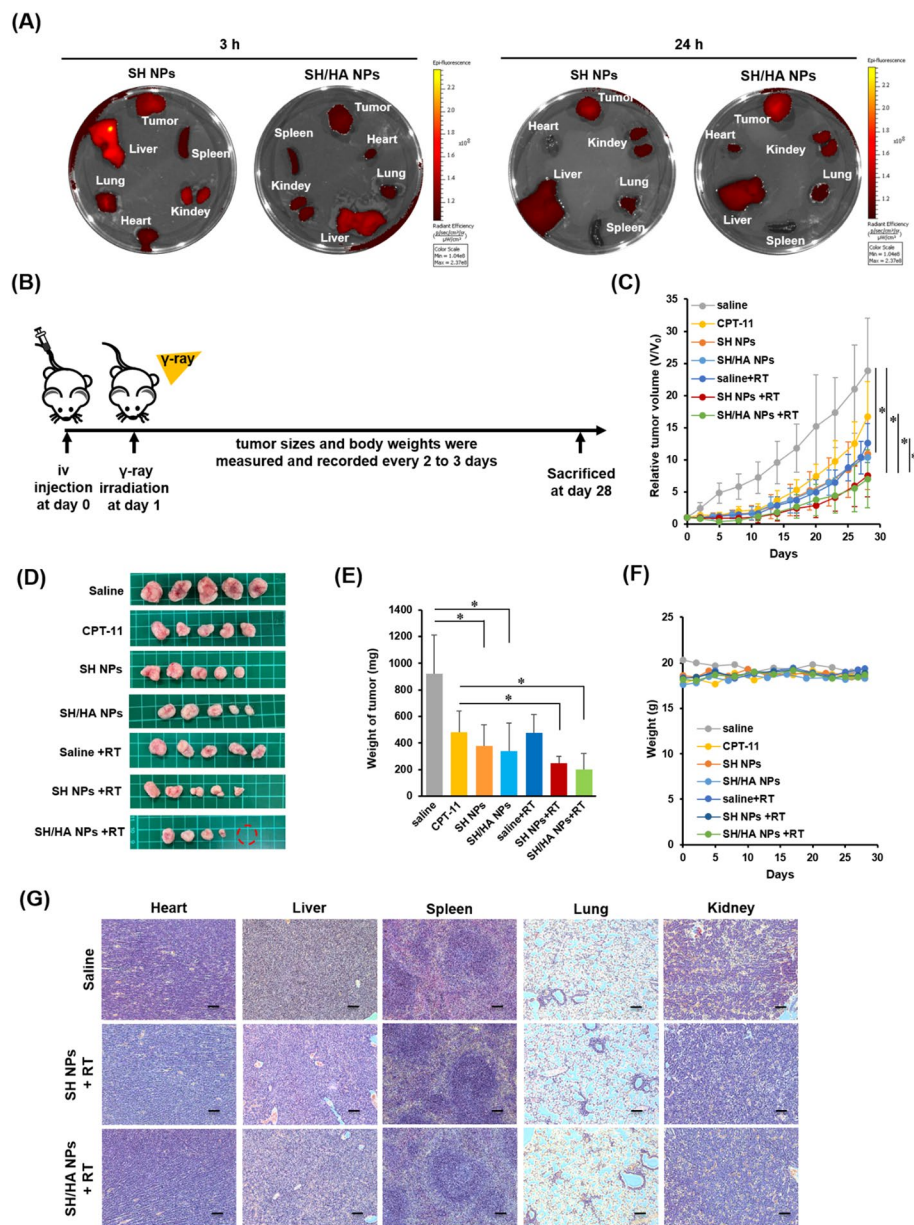
Fig. 5 A Distribution of SH NPs and SH/HA NPs in the main organs and HT29 tumors at 3 and 24 h. **B** Schematic diagram of the treatment of HT29 tumor-bearing mice. **C** Relative primary tumor volumes, **D** representative primary tumor images, and **E** primary tumor weight, and **F** body weights of nude mice treated with saline, CPT-11, SH NPs, and SH/HA NPs with or without γ-ray irradiation (6 Gy) ($n = 5$). **G** H&E stained images of the heart, liver, spleen, lung, and kidney in mice after treatment with saline, SH NPs, and SH/HA NPs plus 6 Gy of γ-ray at 28 days. Scale bar = 200 μm. $*p < 0.05$

to recognize the CD44 molecules on HT29 tumor cells. This results indicated that SH/HA NPs could be more easily accumulated in the tumor, which might be beneficial to produce a better chemo-radiotherapeutic effect.

The primary tumor volume changes of mice pre-treated with saline, free CPT-11, SH NPs, and SH/HA NPs with or without γ-ray irradiation were used to assess therapeutic effects (Fig. 5B). As shown in Fig. 5C, compared with the saline-treated mice, the

CPT-11-treated mice showed an effective inhibition on tumor growth, and the SH NPs and SH/HA NPs treatments also showed a significant suppression on tumor growth. Moreover, the prepared nanoparticles followed by 6 Gy of γ-ray irradiation were more efficient in inhibiting tumor growth, especially for the SH/HA NPs-treated group, which could even completely eliminate tumor tissues (tumor clearance rate was 20%). The photographs of the excised tumors and weights after different treatments indicated that SH/HA NPs followed by γ-ray irradiation could suppress tumor growth and promote higher anticancer efficacy (Fig. 5D, E). The body weight change is the main observation related to survival and treatment response (Marinho et al. 2001). Herein, no significant weight loss was detected for any experimental group over the whole experimental period (Fig. 5F). In addition, no pathological signs were observed in histological examinations of the main organs of mice that were treated with saline or SH NPs or SH/HA NPs plus γ-ray irradiation (Fig. 5G), indicating that none of these treatments would cause obvious damages in main organs. Therefore, the designed SH/HA NPs acts synergistically with radiotherapy and provides a profound anticancer effect.

Effect of SH/HA NPs plus radiation on immune cell infiltrates

To determine whether the inhibition in distal tumor growth seen following chemo-radiotherapy was caused by the induced immune cell response, the effect of CPT-11, SH NPs and SH/HA NPs plus γ-ray irradiation on immune cell infiltration in the distal tumor was examined. The distal tumors were excised at 72 h following different treatments and analyzed by flow cytometry (Fig. 6A). The immune markers stained for different immune cells were as follows: $CD19^+$ B cells, $CD11c^+$ dendritic (DC) cells, $F4/80^+$ macrophages, $DX5^+/CD3^-$ natural killer (NK) cells, and $DX5^+/CD3^+$ NKT cells (Tremble et al. 2019). As shown in Fig. 6B, CPT-11 plus radiation only had significant effect on the recruitment of NKT cells; however, SH NPs combined with radiation resulted in a significant increase in DC cells and NKT cells. The treatment of SH/HA NPs followed by γ-ray irradiation on the primary tumor resulted in significantly enhanced recruitment of B cells, DC cells, macrophages, and NKT cells in the distal tumor. Owing to the stronger immune cell response, SH/HA NPs followed by 6 Gy of γ-ray irradiation could display more effective abscopal effects to inhibit distal tumor growth (Fig. 6C, D).

Discussion

To reduce the side effects of chemotherapy drugs entering the environment, and produce therapeutic effects using a low dose of medication, the nanomedicine has many advantages over conventional pharmaceuticals (Orive et al. 2003). HSA possesses numerous and different functional groups that can be employed for chemical modification and as a carrier for hydrophobic chemotherapeutics (Kratz 2008; Sleep 2015). The use of HSA as a nanocarrier for chemotherapy drugs not only can increase the uptake in tumor cells, but also can effectively enhance the biocompatibility and circulation time of drugs in the blood, improving the treatment effect and reducing the side effects (Frei 2011; Kim et al. 2011; Quan et al. 2011; Elsadek and Kratz 2012; Ding et al. 2014; Sheng et al. 2014).

Herein, the hydrophobic drug, SN38 loaded nanoparticles (SH NPs and SH/HA NPs) were developed using a lyophilization–hydration method, which was established for the development of hydrophobic drug-encapsulated micelles in our previous studies (Peng
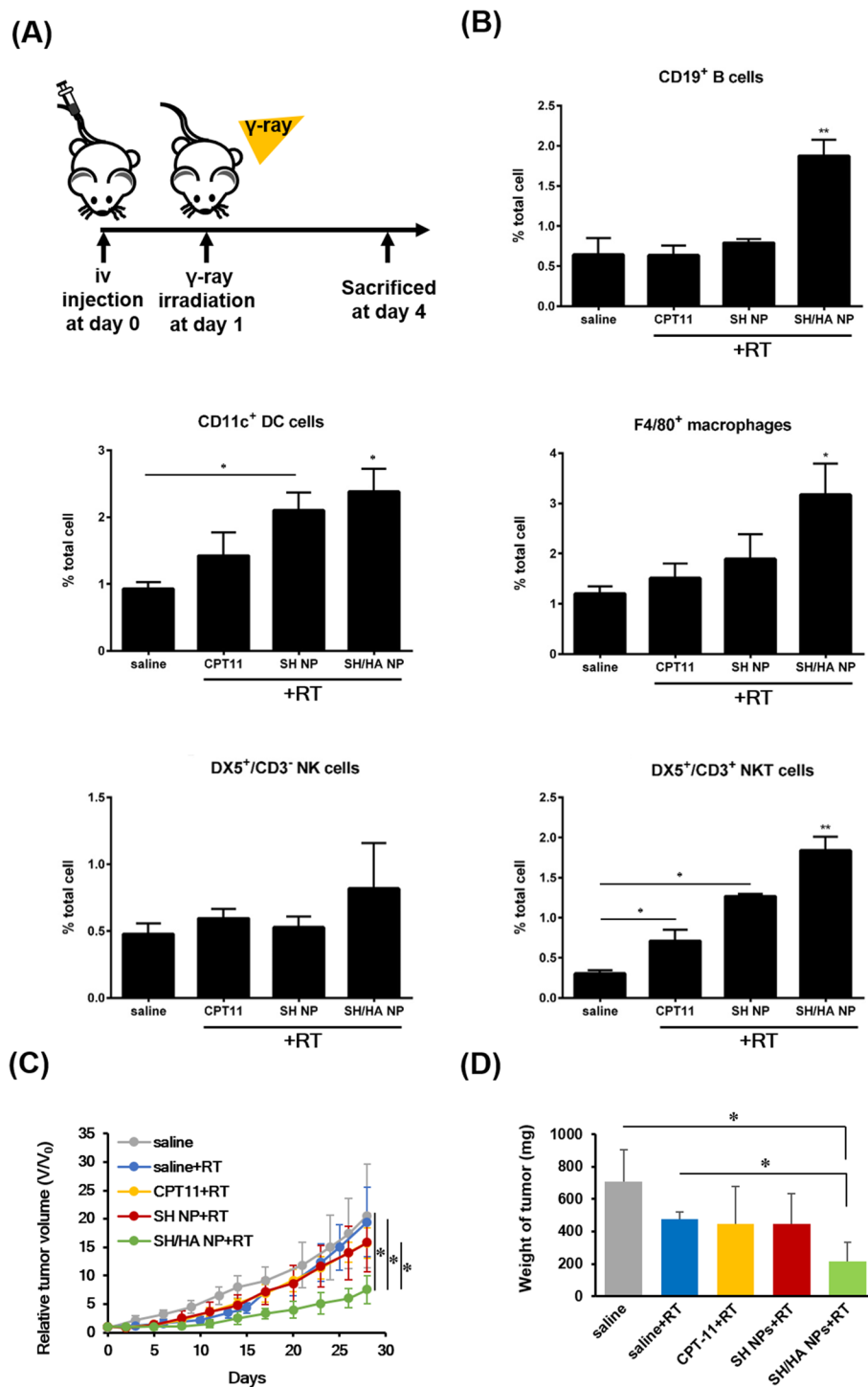
Fig. 6 Abscopal effect on distal HT29 tumors. **A** Schematic diagram of the treatment of HT29 tumor-bearing mice. **B** Intratumoral immune cell infiltration of distal HT29 tumors 72 h post-treatment. Primary HT29 tumors were treated with saline, CPT-11, SH NPs, and SH/HA NPs plus 6 Gy of γ-ray, and the distal tumors were excised and analyzed for the relative abundance of different tumor-infiltrating immune cells by flow cytometry. Cells were gated appropriately to distinguish CD19^{+} B cells, CD11c^{+} DC cells, F4/80^{+} macrophages, DX5^{+}/CD3^{−} NK cells, and DX5^{+}/CD3^{+} NKT cells ($n = 5$). **C** Relative distal tumor volume and **D** tumor weight treated with saline, free CPT-11, SH NPs, and SH/HA NPs plus γ-ray irradiation (6 Gy) at 28 days ($n = 5$). *$p < 0.05$. **$p < 0.01$

et al. 2008; Tsai et al. 2017). Figure 1 not only indicates the encapsulation of SN38 in HSA-based nano-particles was successful, but also the size of prepared nanoparticles was smaller than 200 nm, which was suitable for delivery of an adequate dose and thus, induction of the most efficient therapeutic effect (Kobayashi et al. 2013). Moreover, the disappearance of sharp peaks in the diffraction pattern of SH NPs or SH/HA NPs indicated that SN38 molecules displaying as small crystals or in an amorphous state were well-distributed in HSA-based nanoparticles. The small crystals or amorphous state of SN38 molecules might contribute to produce a higher dissolution rate to obtain a better bioavailability in clinical applications (Hu et al. 2015). In addition, the lyophilized SH NPs and SH/HA NPs was stable in storage for 30 days at 4 °C, which is a key factor that must be considered in the design and development of the pharmaceutical formulation (Gradauer et al. 2013).

In order for cancer cell invasion to be successful, cancer cells have to interact, modify, and pass through the extracellular matrix to proliferate and establish colonies in new ectopic locations (Chambers et al. 2002). CD44 is a unique adhesion molecule, which can promote interactions between cells and the cellular matrix (Subramaniam et al. 2007). Many CD44 splice variants are significantly overexpressed in malignancies, indicating that the overexpression of specific splice variant subtypes of CD44 is associated with the occurrence of metastasis (Günthert et al. 1991). Therefore, the aberrant expression and dysregulation of CD44 contribute to modulate cancer proliferation, invasion, metastasis and therapy-resistance during anti-tumor administration (Xu et al. 2020). Recently, HA has been employed to achieve CD44-regulated tumor target therapy (Cadete and Alonso 2016; Jiang et al. 2021; Hu et al. 2020). In this present study, the HA incorporation should increase the uptake of nanoparticles (SH/HA NPs) in CD44-expressing cells and then improve the elimination of CD44-expressing cells after radiation treatment. Figure 2 shows the prepared nanoparticle cellular uptake was positive relationship with CD44 expression. The highly expressing CD44 molecules in HT29 and HCT116 cells resulted in high activity of the HA-mediated recognition of SH/HA NPs to CD44 on HT29 or HCT116 cells in comparison with that on SW620 cells. In addition, the internalization of SH/HA NPs into HT29 or HCT116 cells could be significantly suppressed by the excessive free HA molecules, indicating that the incorporated HA could mediate the targeting activity of SH/HA NPs to CD44 receptor, and then enhance the CD44-mediated cellular uptake of SH/HA NPs. These results also indicated that incorporated HA in SH/HA NPs as same as free HA molecules could still preserve its targeting and binding activities to CD44 receptor via four conventional H-bond, two carbon H-bond interaction, and a hydrophobic interaction (Sargazi et al. 2018). Moreover, the HA incorporation could mediate the recognition of SH/HA NPs to CD44 molecules on HT29 cell surface, especially for that at a low SN38 concentration (5 ng/mL), resulting in more cytotoxicity than that of SH NPs. Because the CD44 low-expressing SW620 cells exhibited more sensitization to SN-38 toxicity than did by CD44-enriched HT29 cells, resulting in the cytotoxicity of SH/HA NPs on SW620 cells was regardless of tumoral recognition via HA-CD44.

The therapeutic effect of radiation can be enhanced by regulating and controlling the cell cycle of cancer cells in the G2/M phase (Wang et al. 2018; Pawlik and Keyomarsi 2004). Camptothecin-derived drugs possess radiosensitization effects on various cancer

cell lines, by inhibiting the function of DNA topoisomerase I in intracellular DNA repair, leading to significant G2/M phase arrest, followed by increased apoptosis (Wang et al. 2018). SN38 not only is able to specifically target topoisomerase I in the cell nucleus, but also is capable of achieving G2/M cell cycle arrest to make cancer cells more susceptible to the damage caused by radiation (Cliby et al. 2002; Pan et al. 2019). As shown in Fig. 3, the prepared SH NPs and SH/HA NPs could retain the SN38 ability in cancer cells to achieve G2/M phase arrest. In addition, the HA incorporation could mediate the recognition of nanoparticles to CD44 molecules on the tumor cell surface, enhancing the efficiency of nanoparticle uptake in tumor cells and then leading to more cells arresting in the G2/M phase.

The in vitro results shown in Fig. 4 reveal there was no significant cytotoxicity difference in SW620 cells between chemotherapy and combined chemo-radiotherapy. It could be suggested that most of the SW620 cells underwent apoptosis due to the inhibition of DNA topoisomerase I by SN38, but the remaining surviving cells might be resistant to SN38 inhibition, which reduced the ability of cells to enter the G2/M cell cycle phase, making them less sensitive to radiation damage. The similar result also was observed in high-dose SN38 (100 ng/mL) treated HT29 cells. However, the cytotoxic effect of CD44-overexpression cancer cells could be improved by the HSA-complexed and HA-incorporated nanoparticles (SH/HA NPs) combined with radiotherapy.

Because the body natural HA is broken down and resynthesized in the extracellular matrix (ECM) of tissues, it does not affect the delivery of SH/HA NPs in the blood. Figure 5 shows that the particle accumulation in tumor could be enhanced by the HSA-complex and HA-incorporation. The SH/HA NPs would be easily accumulated in the extravascular space of tumors by the enhanced permeability and retention (EPR) effect to offer a prolonged duration of action. The EPR effect due to the hypervascularization and increased vascular permeability in tumor tissues can be exploited for the targeting of macromolecules into tumor tissues (Nakamura et al. 2016). In addition, HSA-complex could avoid capture of SH/HA NPs by the reticuloendothelial system to increase the circulation half-life of nano-carriers in the blood (Elsadek and Kratz 2012; Ding et al. 2014; An and Zhang 2017). When SH/HA NPs were delivered into tumor tissues, the suppress effect of natural HA in the ECM of tumor on the targeting and cellular uptake of SH/HA NPs could be ignored due to the large expression of CD44 receptors on tumor cell surfaces (Günthert et al. 1991). The more SH/HA NPs accumulated and cellular uptaken in the CD44-enriched tumor would provide a better anticancer effect of combined chemo-radiotherapy with low damages in main organs.

The abscopal effect, a phenomenon of radiotherapy, was first observed by Mole in 1953, showing that when radiotherapy was applied to one tumor, non-irradiated tumors also shrank or disappeared, which was considered to be related to the human immune system (Golden et al. 2015). In addition to radiotherapy, the abscopal effect has also been observed after electroporation or intratumoral injection of therapeutics (Kodet et al. 2021). The local radiation can disintegrate tumor cells to release tumor neoantigens. The recognition, intake and presentation of tumor neoantigens to T cells by antigen-presenting cells are mediated by DC cells, inducing a specific anti-tumour immune response (Tel et al. 2014; Demaria et al. 2015). As shown in Fig. 6, the prepared SH NPs or SH/HA NPs combined with γ-ray irradiation could significantly

enhance the recruitment of DC cells, which might induce a strong immune cell response against the distal tumor. In addition to DC cells, the recruitment of macrophages and NKT cells in the distal tumor also were be improved by the SH/HA NPs combined with radiation treatment. NKT cells are T lineage cells that share both physical and functional characteristics of T cells and NK cells and can rapidly respond and mediate potent immunoregulatory and effector functions (Drewes et al. 2014). Although BALB/CAnN.Cg-Foxn1nu/CrlNarl nude mice have a genetic mutation that causes a deteriorated or absent thymus to greatly reduce number of T cells, they still have detectable populations of lymphocytes with the functional αβ T cell receptor expression (Dunn et al. 2002). Therefore, γ-ray irradiation could significantly induce the recruitment of NKT cells in the distal tumor, even in the HT29 tumor-bearing nude mice established in this experiment. Moreover, compared to SH NPs-treated groups, more B cells, macrophages, and NKT cells were recruited in the SH/HA NPs-treated groups, suggested that more SH/HA NPs were accumulated in the CD44-overexpressing tumors to produce a better chemo-radiotherapeutic effect and then induce a stronger immune cell response after radiation treatment. Because the immune system response triggered by chemoradiotherapy is complex and variable, more evaluations are required to perform in the future.

Conclusions

In the present study, SN38, an activated form of CPT-11 with poor water solubility, was successfully encapsulated in HSA–HA-based nanoparticles (SH/HA NPs) via a lyophilization–hydration method to enhance the targeting and cellular uptake in CD44-expressing tumor cells and produce a significant therapeutic effect at a low dose. At the same time, SH/HA NPs could be served as an excellent mediator for radiotherapy to improve the sensitivity of tumor cells to radiation. When combined with γ-ray irradiation, SH/HA NPs due to more accumulation in tumor cells could result in significant tumor suppression with no in vivo adverse side effects. Moreover, this SH/HA NPs-mediated chemo-radiotherapy could induce antitumor immune cell responses and inhibit growth of distal tumors by producing the abscopal effect. Therefore, this SN38-loaded and HA-incorporated nanoparticle may be a potential nanomedicine candidate used in curative colorectal cancer therapy in the future.

Abbreviations

CRC	Colorectal cancer
SN38	7-Ethyl-10-hydroxycamptothecin
HSA	Human serum albumin
HA	Hyaluronic acid
NPs	Nanoparticles
CSCs	Cancer stem cells
SH NPs	SN38-loaded HSA-based nanoparticles
SH/HA NPs	SN38-loaded and HA-incorporated HSA-based nanoparticles
TEM	Transmission electron microscopy
HPLC	High-performance liquid chromatography
XRD	X-ray diffraction
EE	Encapsulation efficacy
DC	Drug-loading content
DCs	Dendritic cells
NK cells	Natural killer cells
NKT cells	Natural killer T cells

Supplementary Information

The online version contains supplementary material available at https://doi.org/10.1186/s12645-022-00151-w.

> **Additional file 1: Figure S1.** Cellular uptake of SH NPs and SH/HA NPs in SW620, HT29, and HCT116 cells with or without 0.1 mg/mL HA pre-treatment.

Author contributions

KCC and MJS contributed to conceptualization and supervision; SJY and JAP were involved in data curation; KCC and MJS contributed to funding acquisition; SJY, JAP, and CJY were involved in investigation; SJY, CHH, LYC, and CHW contributed to methodology; KCC and MJS performed project administration; CHH and CHW did validation; SJY and JAP wrote original draft; KCC and MJS were involved in writing—review and editing. All authors read and approved the final manuscript.

Availability of data and materials

The data sets used and analyzed during the current study are available from the corresponding author on reasonable request.

Declarations

Ethics approval and consent to participate

All animal experiments were performed at Laboratory Animal Center of National Taiwan University College Medicine with prior Institutional Animal Care and Use Committee (IACUC) approval (No. 20190459).

Consent for publication

All authors agree to publish this manuscript in this journal.

Competing interests

The author reports no competing interests in this work.

References

An FF, Zhang XH (2017) Strategies for preparing albumin-based nanoparticles for multifunctional bioimaging and drug delivery. Theranostics 7:3667–3689

Armand JP, Ducreux M, Mahjoubi M, Abigerges D, Bugat R, Chabot G et al (1995) CPT-11 (irinotecan) in the treatment of colorectal cancer. Eur J Cancer 31A(7–8):1283–1287

Attisano L, Wrana JL (2012) The return of Dr Jekyll in cancer metastasis. EMBO J 31:4486–4487

Bala V, Rao S, Boyd BJ, Prestidge CA (2013) Prodrug and nanomedicine approaches for the delivery of the camptothecin analogue SN38. J Control Release 172:48–61

Cadete A, Alonso MJ (2016) Targeting cancer with hyaluronic acid-based nanocarriers: recent advances and translational perspectives. Nanomedicine (lond) 11:2341–2357

Chambers AF, Groom AC, MacDonald IC (2002) Dissemination and growth of cancer cells in metastatic sites. Nat Rev Cancer 2:563–572

Clark J, Sheldon R, Raston C, Poliakoff M, Leitnere W (2014) 15 years of green chemistry. Green Chem 16:18–23

Cliby WA, Lewis KA, Lilly KK, Kaufmann SH (2002) S Phase and G2 arrests induced by topoisomerase I poisons are dependent on ATR kinase function. J Biol Chem 277:1599–1606

Corso CD, Ali AN, Diaz R (2011) Radiation-induced tumor neoantigens: imaging and therapeutic implications. Am J Cancer Res 1:390–412

Demaria S, Golden EB, Formenti SC (2015) Role of local radiation therapy in cancer immunotherapy. JAMA Oncol 1:1325–1332

Ding D, Tang X, Cao X, Wu J, Yuan A, Qiao Q et al (2014) Novel self-assembly endows human serum albumin nanoparticles with an enhanced antitumor efficacy. AAPS PharmSciTech 15:213–222

Drewes JL, Szeto GL, Engle EL, Lia Z, Shearer GM, Zink MC et al (2014) Attenuation of pathogenic immune responses during infection with human and simian immunodeficiency virus (HIV/SIV) by the tetracycline derivative minocycline. PLoS ONE 9:e94375

Dunn GP, Bruce AT, Ikeda H, Old LJ, Schreiber RD (2002) Cancer immunoediting: from immunosurveillance to tumor escape. Nat Immunol 3:991–998

DuRoss AN, Landry MR, Thomas CR Jr, Neufeld MJ, Sun C (2021) Fucoidan-coated nanoparticles target radiation-induced P-selectin to enhance chemoradiotherapy in murine colorectal cancer. Cancer Lett 500:208–219

Elsadek B, Kratz F (2012) Impact of albumin on drug delivery–new applications on the horizon. J Control Release 157:4–28

Frei E (2011) Albumin binding ligands and albumin conjugate uptake by cancer cells. Diabetol Metab Syndr 3:11

Golden EB, Chhabra A, Chachoua A, Adams S, Donach M, Fenton-Kerimian M et al (2015) Local radiotherapy and granulocyte-macrophage colony-stimulating factor to generate abscopal responses in patients with metastatic solid tumours: a proof-of-principle trial. Lancet Oncol 16:795–803

Gradauer K, Dünnhaupt S, Vonach C, Szöllösi H, Pali-Schöll I, Mangge H et al (2013) Thiomer-coated liposomes harbor permeation enhancing and efflux pump inhibitory properties. J Control Release 165:207–215

Günthert U, Hofmann M, Rudy W, Reber S, Zöller M, Haussmann I et al (1991) A new variant of glycoprotein CD44 confers metastatic potential to rat carcinoma cells. Cell 65:13–24

Hu S, Lee E, Wang C, Wang J, Zhou Z, Li Y et al (2015) Amphiphilic drugs as surfactants to fabricate excipient-free stable nanodispersions of hydrophobic drugs for cancer chemotherapy. J Control Release 220(Pt A):175–179

Hu X, Hou B, Xu Z, Saeed M, Sun F, Gao Z et al (2020) Supramolecular prodrug nanovectors for active tumor targeting and combination immunotherapy of colorectal cancer. Adv Sci (weinh) 7:1903332

Jiang M, Li W, Zhu C, Li X, Zhang J, Luo Z et al (2021) Perdurable PD-1 blockage awakes anti-tumor immunity suppressed by precise chemotherapy. J Control Release 329:1023–1036

Kanegasaki S, MatsushimaK SK, Nakagawa K, Tsuchiya T (2014) Macrophage inflammatory protein derivative ECI301 enhances the alarmin-associated abscopal benefits of tumor radiotherapy. Cancer Res 74:5070–5078

Kim TH, Jiang HH, Youn YS, Park CW, Tak KK, Lee S (2011) Preparation and characterization of water-soluble albumin-bound curcumin nanoparticles with improved antitumor activity. Int J Pharm 403:285–291

Kobayashi H, Watanabe R, Choyke PL (2013) Improving conventional enhanced permeability and retention (EPR) effects; what is the appropriate target? Theranostics 4(1):81–89

Kodet O, Němejcova K, Strnadová K, Havlínová A, Dundr P, Krajsová I et al (2021) The abscopal effect in the Era of check-point inhibitors. Int J Mol Sci 22:7204

Kouchakzadeh H, Safavi MS, Shojaosadati SA (2015) Efficient delivery of therapeutic agents by using targeted albumin nano-particles. Adv Protein Chem Struct Biol 98:121–143

Kratz F (2008) Albumin as a drug carrier: design of prodrugs, drug conjugates and nanoparticles. J Control Release 132:171–183

Lam PL, Kok HL, Gambari R, Kok TW, Leung HY, Choi KL et al (2015) Evaluation of berberine/bovine serum albumin nano-particles for liver fibrosis therapy. Green Chem 17:1640–1646

Lee S, Lee C, Park S, Lim K, Kim SS, Kim JO et al (2018) Facile fabrication of highly photothermal-effective albumin-assisted gold nanoclusters for treating breast cancer. Int J Pharm 553:363–374

Magrini R, Bhonde MR, Hanski ML, Notter M, Scherübl H, Boland CR et al (2002) Cellular effects of CPT-11 on colon carci-noma cells: dependence on p53 and hMLH1 status. Int J Cancer 101:23–31

Marinho LA, Rettori O, Vieira-Matos AN (2001) Body weight loss as an indicator of breast cancer recurrence. Acta Oncol 40:832–837

Moreno CC, Mittal PK, Sullivan PS, Rutherford R, Staley CA, Cardona K (2016) Colorectal cancer initial diagnosis: screening colonoscopy, diagnostic colonoscopy, or emergent surgery, and tumor stage and size at initial presentation. Clin Colorectal Cancer 15:67–73

Nakamura Y, Mochida A, Choyke PL, Kobayashi H (2016) Nanodrug delivery: is the enhanced permeability and retention effect sufficient for curing cancer? Bioconjug Chem 27(10):2225–2238

Orive G, Hernández RM, Rodríguez Gascón A, Domínguez-Gil A, Pedraz JL (2003) Drug delivery in biotechnology: present and future. Curr Opin Biotechnol 14:659–664

Pan W, Gong S, Wang J, Yu L, Chen Y, Li N et al (2019) A nuclear-targeted titanium dioxide radiosensitizer for cell cycle regulation and enhanced radiotherapy. Chem Commun (camb) 55:8182–8185

Pawlik TM, Keyomarsi K (2004) Role of cell cycle in mediating sensitivity to radiotherapy. Int J Radiat Oncol Biol Phys 59:928–942

Peng CL, Shieh MJ, Tsai MH, Chang CC, Lai PS (2008) Self-assembled star-shaped chlorin-core poly(epsilon-caprolactone)-poly(ethylene glycol) diblock copolymer micelles for dual chemo-photodynamic therapies. Biomaterials 29:3599–3608

Quan Q, Xie J, Gao H, Yang M, Zhang F, Liu G et al (2011) HSA coated iron oxide nanoparticles as drug delivery vehicles for cancer therapy. Mol Pharm 8:1669–1676

Rivory LP, Bowles MR, Robert J, Pond SM (1996) Conversion of irinotecan (CPT-11) to its active metabolite, 7-ethyl-10-hy-droxycamptothecin (SN-38), by human liver carboxylesterase. Biochem Pharmacol 52:1103–1111

Roger E, Lagarce F, Benoit JP (2011) Development and characterization of a novel lipid nanocapsule formulation of Sn38 for oral administration. Eur J Pharm Biopharm 79:181–188

Sargazi A, Shiri F, Keikha S, Majd MH (2018) Hyaluronan magnetic nanoparticle for mitoxantrone delivery toward CD44-positive cancer cells. Colloids Surf B Biointerfaces 171:150–158

Sheng Z, Hu D, Zheng M, Zhao P, Liu H, Gao D et al (2014) Smart human serum albumin-indocyanine green nanoparti-cles generated by programmed assembly for dual-modal imaging-guided cancer synergistic phototherapy. ACS Nano 8:12310–12322

Sleep D (2015) Albumin and its application in drug delivery. Expert Opin Drug Deliv 12:793–812

Subramaniam V, Vincent IR, Gardner H, Chan E, Dhamko H, Jothy S (2007) CD44 regulates cell migration in human colon cancer cells via Lyn kinase and AKT phosphorylation. Exp Mol Pathol 83:207–215

Tel J, Anguille S, Waterborg CE, Smits EL, Figdor CG, de Vries IJ (2014) Tumoricidal activity of human dendritic cells. Trends Immunol 35:38–46

Tirkey B, Bhushan B, Uday Kumar S, Gopinath P (2017) Prodrug encapsulated albumin nanoparticles as an alternative approach to manifest anti-proliferative effects of suicide gene therapy. Mater Sci Eng C Mater Biol Appl 73:507–515

Tremble LF, O'Brien MA, Soden DM, Forde PF (2019) Electrochemotherapy with cisplatin increases survival and induces immunogenic responses in murine models of lung cancer and colorectal cancer. Cancer Lett 2442:475–482

Tsai MH, Peng CL, Yang SJ, Shieh MJ (2017) Photothermal, targeting, theranostic near-infrared nanoagent with SN38 against colorectal cancer for chemothermal therapy. Mol Pharm 14:2766–2780

Venditto VJ, Szoka FC Jr (2013) Cancer nanomedicines: so many papers and so few drugs! Adv Drug Deliv Rev 65:80–88

Wang D, Gao Y, Lin Z, Yao Z, Zhang W (2014) The joint effects on photobacterium phosphoreum of metal oxide nanoparticles and their most likely coexisting chemicals in the environment. Aquat Toxicol 154:200–206

Wang Y, Yang L, Zhang J, Zhou M, Shen L, Deng W et al (2018) (2018) Radiosensitization by irinotecan is attributed to G2/M phase arrest, followed by enhanced apoptosis, probably through the ATM/Chk/Cdc25C/Cdc2 pathway in p53-mutant colorectal cancer cells. Int J Oncol 53:1667–1680

Xu H, Niu M, Yuan X, Wu K, Liu A (2020) CD44 as a tumor biomarker and therapeutic target. Exp Hematol Oncol 9(1):36

Yang SJ, Huang CH, Wang CH, Shieh MJ, Chen KC (2020) The synergistic effect of hyperthermia and chemotherapy in magnetite nanomedicine-based lung cancer treatment. Int J Nanomedicine 15:10331–10347

Yang SJ, Huang HT, Huang CH, Pai JA, Wang CH, Shieh MJ (2022) The synergistic effect of chemo-photothermal therapies in SN-38-loaded gold-nanoshell-based colorectal cancer treatment. Nanomedicine (lond) 17(1):23–40

Yin T, Wang G, He S, Liu Q, Sun J, Wang Y (2016) Human cancer cells with stem cell-like phenotype exhibit enhanced sensitivity to the cytotoxicity of IL-2 and IL-15 activated natural killer cells. Cell Immunol 300:41–45

Zhang JA, Xuan T, Parmar M, Ma L, Ugwu S, Ali S et al (2004) Development and characterization of a novel liposome-based formulation of SN-38. Int J Pharm 270:93–107

Zhang YN, Poon W, Tavares AJ, McGilvray ID, Chan WCW (2016) Nanoparticle-liver interactions: Cellular uptake and hepatobiliary elimination. J Control Release 240:332–348

Publisher's Note